State of Charge Estimation for Lithium-Ion Batteries Using Neural Networks and Extended Kalman Filter

***Abstract*—This paper presents a method for modeling and estimation of the State Of Charge (SOC) of lithium-ion batteries using neural networks and the Extended Kalman Filter (EKF). The neural network is trained off-line using the data collected from the battery charging process. This network finds the model needed in the state space equations of the EKF, where the state variables are the battery terminal voltage at the previous sample and the SOC at the present sample. Furthermore, the covariance matrix for the process noise in EKF is estimated adaptively. The proposed method is implemented on a lithium-ion battery to on-line estimate the actual SOC of the battery. Experimental results show good estimation of SOC and fast convergence of the EKF state variables.**

***Index Terms*: Batteries, monitoring, estimation, Kalman filtering, neural networks.**

I. Introduction

SOME BATTERIES are sensitive to overcharge and/or deep discharge, which may lead to permanent damage to these devices. In the charging process, it is usually desirable to charge the battery with the highest and safest current in order to reach the full State of Charge (SOC) as quickly as possible without entering the overcharge region [1], [2]. Therefore, it is necessary to measure the SOC with good accuracy for proper battery managements. Moreover, the State of Health (SOH) of batteries requires maintaining the SOC within certain limits at all times [2], [3].

The SOC definition, in the simplest way, is the ratio between the saved energy in the battery and the whole energy that can be saved in it [2]. The SOC estimation is not an easy task and depends on the battery type and the applications for which they are used. Generally, there are two categories for SOC estimation: indirect methods and direct methods. In indirect methods, the SOC is estimated from some physical properties of the battery, such as the acid density or the cathodic galvanostatic pulses. Estimating these quantities needs precise measurements and has several limitations in practice [2], [4]. The other indirect method is measuring the open-circuit voltage of the battery. In this method, the battery must be relaxed for some time to allow its open-circuit voltage reach a steady-state condition. Therefore, this method is not practical in applications where the battery is not allowed to be opened from the electric circuit [2], [5]. In other methods, SOC is estimated using the discharge voltage of the battery [6]. Impedance spectroscopy is a commonly used indirect method for electrochemical processes such as batteries. This method is used not only for the SOC estimation but also for the SOH estimation as well [7], [8]. However, this approach requires some additional measurements that make it suitable in laboratory tests, but not in practical applications [2]. In [9] the battery impedance is measured directly through varying frequency to improve the charging process. In [10], the electromotive force voltage is estimated, from which the SOC of the battery is determined. In this work, it is necessary to measure the battery impedance with ac current and voltage, which seems to be suitable for laboratory tests.

Some researchers have used fuzzy logic to model the relationship between the battery SOC and its parameters derived from impedance spectroscopy measurements [11], [12]. Among the direct methods for SOC estimation is the Ampere-hour counting technique. This method needs the initial SOC, calculation of the internal consumptions by the battery, and accurate current sensors [13]. Artificial neural networks have also been used by some researchers for the SOC estimation [14]-[19]. In this method, there is need for some input-output data as the training set, which must be obtained by some other estimation methods. The trained network can then be used to estimate the SOC.

The Kalman filter is a powerful tool for the state estimation of systems. Some researchers have used this filter to estimate the open-circuit voltage or other parameters of batteries that have a direct relationship with the SOC [20], [23]. In [24] and [25], the Kalman filter is employed to estimate some physical quantities, which have direct effects on the SOC. In some papers, the SOC is defined as a model state and is estimated using the Kalman filter [3], [26]-[28]. However, the Kalman filter needs a suitable model of the battery. Moreover, due to the use of feedbacks in this filter, there is need for proper initialization of states; otherwise, its states may not converge.

In this paper, a state-space model of the SOC is proposed that is approximated using a neural network. Then, using the Extended Kalman Filter (EKF) along with the proposed model, the battery SOC is estimated. The proposed method is implemented and tested on a Li-Ion battery. The experimental results show good accuracy and quick convergence for estimating the SOC of lithium-ion batteries.

This paper is organized as follows. Section 2 describes the battery model. Section 3 presents the proposed SOC estimation algorithm. Section 4 shows the experimental setups and results. Finally, section 5 draws some conclusions and gives directions for the future work.

II. MODELING

In this paper, the SOC is defined as an independent state-space variable and is modeled using a Radial Basis Function (RBF) neural network [29].

A. SOC as the state space variable

The SOC can be defined as the ratio between the saved energy in a battery and the whole energy that could be saved in it [2, 26]

$$z(t) = z(t_0) + \int_{t_0}^{t} \frac{\eta_i \, i(\tau)}{C_n} d\tau \tag{1}$$

where $z(t)$ is the SOC, $z(t_0)$ is the initial SOC, C_n is the nominal capacity, $i(t)$ is the instantaneous current (positive for discharge and negative for charge), η_i is the Columbic efficiency ($\eta_i = 1$ for discharge and $\eta_i = \eta \le 1$ for charge) [26].

In order to employ the Kalman filter, it is necessary to discretize the model given in (1). Assuming that the sampling rate Δt is small enough and substituting the integral with the Euler approximation, Eq. (1) can be written as

$$z(k+1) = z(k) + \frac{\eta_i \, \Delta t}{C_n} i(k) \tag{2}$$

As Eq. (2) shows, the SOC is defined as an independent state variable in the state space model. Other state variables and the output equation will be given in the next section.

B. The proposed model

The SOC of batteries has a nonlinear relationship with its terminal voltage and current [27]. It is usually not an easy task to obtain this nonlinear relationship. One way to find this relationship is to analyze the chemical reaction equations, which is very complicated. Fortunately, neural networks are universal approximators and can approximate any nonlinear function with desired accuracies [29]. In this paper, a RBF network is used to find the required nonlinear model. Fig.1 shows the structure of an RBF network, where the inputs are the battery voltage at step *k*-1, the estimated SOC at step *k*, and the battery terminal current at step *k*. The output of the neural network approximates the battery terminal voltage at step *k*. In this network, the activation functions of neurons in the hidden layer are Green functions (e.g. Gaussian functions) in the following form:

$$\varphi_i(\mathbf{r}_k) = G\left(\left\|\mathbf{r}_k - \mathbf{t}_i\right\|\right) = \exp\left(-\left\|\mathbf{r}_k - \mathbf{t}_i\right\|^2 \Big/ \sigma_i^2\right), \quad i = 1, \ldots, M \tag{3}$$

where $\mathbf{r}_k = \left[v(k-1) \quad z(k) \quad i(k)\right]^T$ is the input vector applied to the network at the kth step, $\mathbf{t}_i$ and σ_i are the center and the standard deviation of the Gaussian function, respectively, and M is the number of neurons in the hidden layer. In fact, the output of this neural network (i.e. the battery terminal voltage at step *k*) is the sum of the weighted Gaussian functions as

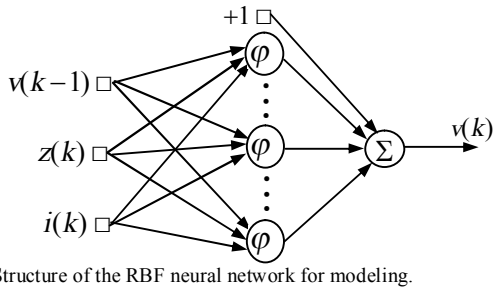

Fig. 1. Structure of the RBF neural network for modeling.

$$F(\mathbf{r}_k) = w_0 + \sum_{i=1}^{M} w_i \, \varphi_i(\mathbf{r}_k) \tag{4}$$

where w_i ($i = 1, \ldots, M$) is the weight vector connecting the ith neuron in the hidden layer to the output layer and w_0 is the bias weight for the linear output neuron. The free parameters of this network are $\mathbf{t}_i$, σ_i, w_i, and w_0, which are defined during the training phase of the network using algorithms such as the back-propagation and the least mean square [29].

Considering the battery terminal voltage at step $k-1$ and the SOC at step k as the first and the second state variables, respectively, the state vector is defined as

$$\mathbf{x}_k =: \begin{bmatrix} x_1(k) \\ x_2(k) \end{bmatrix} = \begin{bmatrix} v(k-1) \\ z(k) \end{bmatrix} \Rightarrow \mathbf{x}_{k+1} = \begin{bmatrix} x_1(k+1) \\ x_2(k+1) \end{bmatrix} = \begin{bmatrix} v(k) \\ z(k+1) \end{bmatrix} \tag{5}$$

where v and z represent the terminal voltage and the SOC of battery, respectively. Using the above definition as the state vector, the state space model can be defined in the following form:

$$\begin{aligned} \begin{bmatrix} x_1(k+1) \\ x_2(k+1) \end{bmatrix} &= \begin{bmatrix} F(\mathbf{r}_k) \\ x_2(k) + \dfrac{\eta_i \, \Delta t}{C_n} i(k) \end{bmatrix} + \begin{bmatrix} \omega_1(k) \\ \omega_2(k) \end{bmatrix} \\ \begin{bmatrix} y_1(k) \\ y_2(k) \end{bmatrix} &= \begin{bmatrix} F(\mathbf{r}_k) \\ x_1(k) \end{bmatrix} + \begin{bmatrix} \upsilon_1(k) \\ \upsilon_2(k) \end{bmatrix} \end{aligned} \tag{6}$$

where $F(\mathbf{r}_k)$ is a nonlinear function, which will be approximated by the RBF network, vectors $\boldsymbol{\omega} = \left[\omega_1 \quad \omega_2\right]^T$ and $\boldsymbol{\upsilon} = \left[\upsilon_1 \quad \upsilon_2\right]^T$ are defined as the process and the measurement noises, respectively, with covariance matrices

$$\begin{aligned} E[\boldsymbol{\omega}_k \, \boldsymbol{\omega}_k^T] &= \mathbf{Q}_k \\ E[\boldsymbol{\upsilon}_k \, \boldsymbol{\upsilon}_k^T] &= \mathbf{R}_k \end{aligned} \tag{7}$$

Moreover, $\mathbf{r}_k$ (i.e. the input vector to the neural network) is defined as

$$\mathbf{r}_k =: \left[\mathbf{x}_k^T \quad i_k\right]^T \tag{8}$$

where $\mathbf{x}_k$ is given in (5). Notice that, in the proposed model, the terminal voltage of battery at steps k and $k-1$, which are shown in the output equations as $y_1(k)$ and $y_2(k)$, respectively, are used in the proposed model.

III. Estimation Algorithm

The estimation algorithm, in this paper, is based on the extended Kalman filter. The performance of Kalman filters depends on several factors, among them, dependency on an accurate state space model of the system, which was proposed in the previous section.

A. Extended Kalman filter

The Kalman filter that is estimating the states of a linear time-varying model, which approximates the nonlinear model, is called the Extended Kalman Filter (EKF). Hence, if the system, whose states are to be estimated by the EKF, has a nonlinear model, then the nonlinear system must be linearized first around the operating point with a time-varying approximation. Even though the performance of EKF is not optimal, it works fine for most applications [30]. For convenience, a summary of the EKF algorithm is given in Table 1.

One important issue in designing a Kalman filter is the proper selection of covariance matrices for measurement and process noises. The covariance matrix of the measurement noise (**R**) can be determined from the battery data. The variances can be obtained from the square of the root-mean-square (RMS) of noisy measurements on the battery terminal voltage. Moreover, it is assumed that the variances are independent and have Gaussian distributions [21]. The covariance matrix of the process noise (**Q**) is estimated in this paper using the Maybeck's estimator as [31]

$$\hat{\mathbf{Q}}(k)=\frac{1}{N}\sum_{j=k-N+1}^{K}\left[\mathbf{G}_j\mathbf{v}_j\mathbf{v}_j^T\mathbf{G}_j^T-\left(\mathbf{A}_{j-1}\mathbf{P}_{j-1}\mathbf{A}_{j-1}^T-\mathbf{P}_j\right)\right] \quad (10)$$

where matrices **G**, **A** and **P** are given in Table 1, N is the number of recent sample periods and $\mathbf{v}$ is the innovation vector calculated as

$$\mathbf{v}_j=\mathbf{y}_j-\mathbf{h}\left(\hat{\mathbf{x}}_j^-,\mathbf{u}\right) \quad (11)$$

B. Linearizing the Proposed Model

In order to apply the EKF to the proposed nonlinear model in (6), the battery model must be linearized at sampling instants. Let define the nonlinear transition matrix function $\mathbf{f}(\mathbf{x}_k,\mathbf{u}_k)$ and the nonlinear measurement matrix $\mathbf{h}(\mathbf{x}_k,\mathbf{u}_k)$ as

$$\mathbf{f}(\mathbf{x}_k,\mathbf{u}_k)=:\begin{bmatrix}F(\mathbf{r}_k)\\ x_2(k)+\left(\eta_i\,\Delta t\,i_k/C_n\right)\end{bmatrix},\ \mathbf{h}(\mathbf{x}_k,\mathbf{u}_k)=:\begin{bmatrix}F(\mathbf{r}_k)\\ x_1(k)\end{bmatrix} \quad (12)$$

Differentiating $\mathbf{f}(\mathbf{x}_k,\mathbf{u}_k)$ and $\mathbf{h}(\mathbf{x}_k,\mathbf{u}_k)$ with respect to $\mathbf{x}_k$ and then letting $\mathbf{x}_k=\hat{\mathbf{x}}_k$ and $\mathbf{x}_k=\hat{\mathbf{x}}_k^-$, respectively, yields

$$\mathbf{A}_k=\begin{bmatrix}\partial F(\mathbf{r}_k)/\partial\mathbf{x}_k\\ 0\quad 1\end{bmatrix}_{\mathbf{x}_k=\hat{\mathbf{x}}_k},\quad \mathbf{C}_k=\begin{bmatrix}\partial F(\mathbf{r}_k)/\partial\mathbf{x}_k\\ 1\quad 0\end{bmatrix}_{\mathbf{x}_k=\hat{\mathbf{x}}_k^-} \quad (13)$$

where $F(\mathbf{r}_k)$ is the output of the RBF network. Hence,

$$\frac{\partial F(\mathbf{r}_k)}{\partial\mathbf{x}_k}=\sum_{i=1}^{M}w_i\frac{\partial\varphi\left(\|\mathbf{r}_k-\mathbf{t}_i\|\right)}{\partial\mathbf{x}_k}, \quad (14)$$

Table 1: Summary of the EKF algorithm.

State space model

$$\mathbf{x}_{k+1}=\mathbf{f}(\mathbf{x}_k,\mathbf{u}_k)+\boldsymbol{\omega}_k$$
$$\mathbf{y}_k=\mathbf{h}(\mathbf{x}_k,\mathbf{u}_k)+\boldsymbol{\upsilon}_k$$

where $\boldsymbol{\omega}_k$ and $\boldsymbol{\upsilon}_k$ are independent, zero mean, Gaussian process and measurement noises with covariance matrices $\mathbf{Q}_k=E[\boldsymbol{\omega}_k\ \boldsymbol{\omega}_k^T]$ and $\mathbf{R}_k=E[\boldsymbol{\upsilon}_k\ \boldsymbol{\upsilon}_k^T]$, respectively.

Definition

$$\mathbf{A}_k=\left.\frac{\partial\mathbf{f}(\mathbf{x}_k,\mathbf{u}_k)}{\partial\mathbf{x}}\right|_{\mathbf{x}=\hat{\mathbf{x}}_k},\quad \mathbf{C}_k=\left.\frac{\partial\mathbf{h}(\mathbf{x}_k,\mathbf{u}_k)}{\partial\mathbf{x}}\right|_{\mathbf{x}=\hat{\mathbf{x}}_k^-}$$

Initialization

$$\hat{\mathbf{x}}_0=E[\mathbf{x}_0],$$
$$\mathbf{P}_0=E\left[\left(\mathbf{x}_0-E[\mathbf{x}_0]\right)\left(\mathbf{x}_0-E[\mathbf{x}_0]\right)^T\right]$$

Calculate for $k=1,2,\ldots$

Time update

State estimate propagation

$$\hat{\mathbf{x}}_k^-=\mathbf{f}(\hat{\mathbf{x}}_{k-1},\mathbf{u}_{k-1})$$

Error covariance propagation

$$\mathbf{P}_k^-=\mathbf{A}_{k-1}\mathbf{P}_{k-1}\mathbf{A}_{k-1}^T+\mathbf{Q}_{k-1}$$

Measurement update

Kalman gain matrix

$$\mathbf{G}_k=\mathbf{P}_k^-\mathbf{C}_k^T(\mathbf{C}_k\mathbf{P}_k^-\mathbf{C}_k^T+\mathbf{R}_k)^{-1}$$

State estimate update

$$\hat{\mathbf{x}}_k=\hat{\mathbf{x}}_k^-+\mathbf{G}_k\left[\mathbf{y}_k-\mathbf{h}(\hat{\mathbf{x}}_k^-,\mathbf{u}_k)\right]$$

Error covariance update

$$\mathbf{P}_k=(\mathbf{I}-\mathbf{G}_k\mathbf{C}_k)\mathbf{P}_k^-$$

in which, the derivative of $\partial\varphi\left(\|\mathbf{r}_k-\mathbf{t}_i\|\right)$ with respect to $\mathbf{x}_k$ can be found using (3) as

$$\frac{\partial\varphi\left(\|\mathbf{r}_k-\mathbf{t}_i\|\right)}{\partial\mathbf{x}_k}=\left(\frac{\partial\varphi\left(\|\mathbf{r}_k-\mathbf{t}_i\|\right)}{\partial\mathbf{r}_k}\right)^T\frac{\partial\mathbf{r}_k}{\partial\mathbf{x}_k} \quad (15)$$

Then, using $\mathbf{r}_k=:\begin{bmatrix}x_1(k) & x_2(k) & i_k\end{bmatrix}^T$, it yields

$$\frac{\partial\mathbf{r}_k}{\partial\mathbf{x}_k}=\begin{bmatrix}1&0\\0&1\\0&0\end{bmatrix} \quad (16)$$

Moreover, assuming $\varphi(\cdot)$ is a Gaussian function as in (3), it gives

$$\frac{\partial\varphi\left(\|\mathbf{r}_k-\mathbf{t}_i\|\right)}{\partial\mathbf{r}_k}=-\frac{2}{\sigma_i^2}\varphi\left(\|\mathbf{r}_k-\mathbf{t}_i\|\right)\cdot(\mathbf{r}_k-\mathbf{t}_i) \quad (17)$$

Substituting (15), (16) and (17) into (14) yields

$$\frac{\partial F(\mathbf{r}_k)}{\partial\mathbf{x}_k}=-\frac{2}{\sigma_i^2}\sum_{i=1}^{M}w_i\varphi\left(\|\mathbf{r}_k-\mathbf{t}_i\|\right)\cdot(\mathbf{r}_k-\mathbf{t}_i)^T\cdot\frac{\partial\mathbf{r}_k}{\partial\mathbf{x}_k} \quad (18)$$

IV. Implementation and Experimental Setup

The proposed SOC estimator is tested on a lithium-ion battery. Fig. 2 shows the general structure of the experimental setup. The hardware consists of a special interface circuit for sampling the current, the voltage, and the batter temperature. The sampled data are transferred to a computer via the serial port. The programming language for data manipulation and processing is Visual C++. In addition, for acquiring data for training the RBF neural network and for testing the proposed SOC estimator, a battery charger has been included that controls the on-off time of charging and discharging the battery. The charging technique is based on the reflex charging method, which is considered as one of the most effective charging schemes [32]. In this charging method, the battery is first charged with a constant current for a small period of time, followed by discharging for a very short time and a relax interval at the end. The entire charging process can be viewed on the computer monitor (Fig. 2).

Fig. 3, 4, and 5 show the designed circuits for the sampling interface, the signal conditioning, and the controllable charger, respectively. As Fig. 3 shows, microcontroller 89C52 is used to transfer the sampled voltage, current, and temperature of battery to the computer. Moreover, this microcontroller controls the on-off time of charging and discharging by applying the appropriate inputs to the driver, based on the given commands by the computer.

For the temperature sensing, an LM35 sensor is used. This sensor is calibrated in Kelvin and has 10 mV/˚C scale factor. In the proposed method, the battery temperature plays no role in the charging process. It is shown only for monitoring purposes. The entire experimental setup is carried out at room temperature. For the current sensing, since the maximum current of the charger is set to about 1.5 A, a 0.1 ohm 5W resistor is used. Moreover, for voltage sensing, a differential amplifier is employed. For data sampling, the ADC0809 is used. This chip has a resolution of 8 bit and can convert analog inputs to discrete outputs in less than 50μs. For sampling, the analog input in all 8 channels must be in the range of 0 to 5V. Hence, it is necessary to use a signal adaptor to match the sensors outputs with the analog inputs of ADC0809 through the signal conditioning circuits (Fig. 4).

Fig. 5 shows the controllable charger, designed for acquiring the data as well as testing the proposed technique for the SOC estimation. The charger consists of a current source and a discharging 3.9Ω/5W resistor used as a load. These two circuits are controlled by the SW1 and SW2 inputs, respectively. Since Li-Ion batteries are very sensitive to voltages above their nominal voltages, a voltage regulator is designed to maintain the battery terminal voltage at 4.2V. This voltage regulator consists of Q6, Q7, OP07, and LM317 (Fig. 5).

A. Battery SOC Estimation

As it was mentioned in Section 2, the battery is modeled using an RBF neural network, which is trained using the data obtained from the battery. Since the SOC of the battery is one of the inputs to the neural network, it is necessary to measure

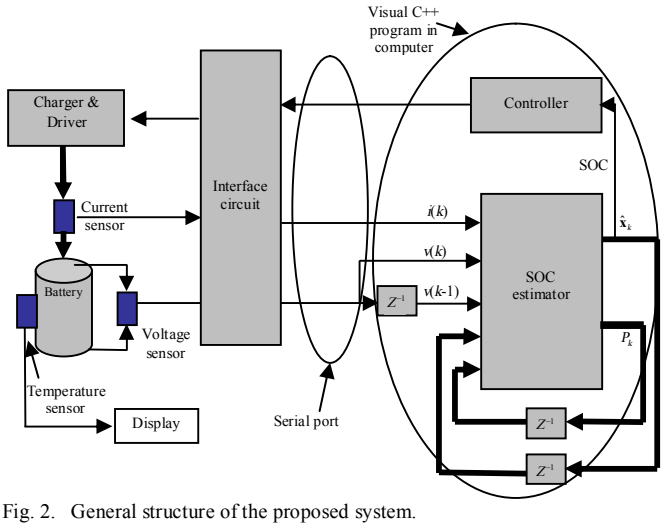

Fig. 2. General structure of the proposed system.

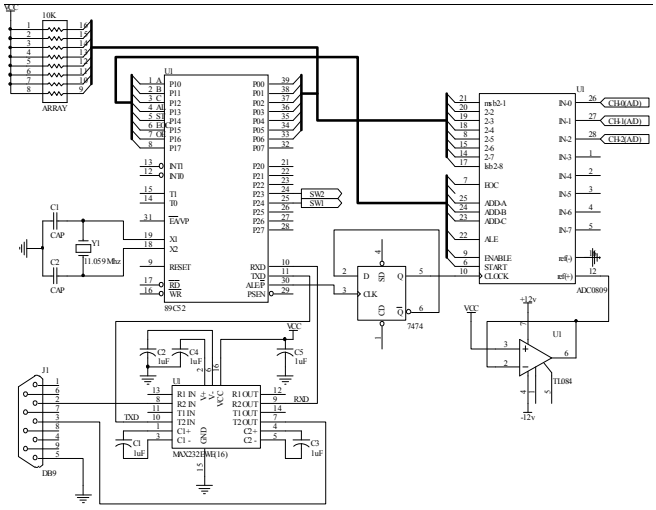

Fig. 3. Interfacing and sampling circuits.

the SOC using one of the available methods. For this reason, the Ampere-hour counting technique, given in (2), is employed for collecting the training data. For calculating η_i, the energy delivered by the battery during discharging is divided by the rated energy (the nominal capacity) of the battery C_n. Moreover, the sampling period Δt is equal to 0.8 second for the SOC estimation. It should be mentioned that the sampling rate of the experimental setup is 50 ms, which is used for display purposes, but the SOC estimation process is updated every 800 ms.

Fig. 6 shows the data acquired from the experimental test on a 1.2 Ah lithium-ion battery. These data are used for training of the RBF network. Although the battery temperature is measured and saved here, it is not used for the estimation or charging processes; the experiments have been carried out at room temperature.

The covariance matrix $\mathbf{R}$ is determined from the data in Fig. 6, based on the square of the rms error between the actual and noisy terminal voltage, and is equal to $\mathbf{R} = \mathrm{diag}\left[0.01 \quad 0.01\right]$.

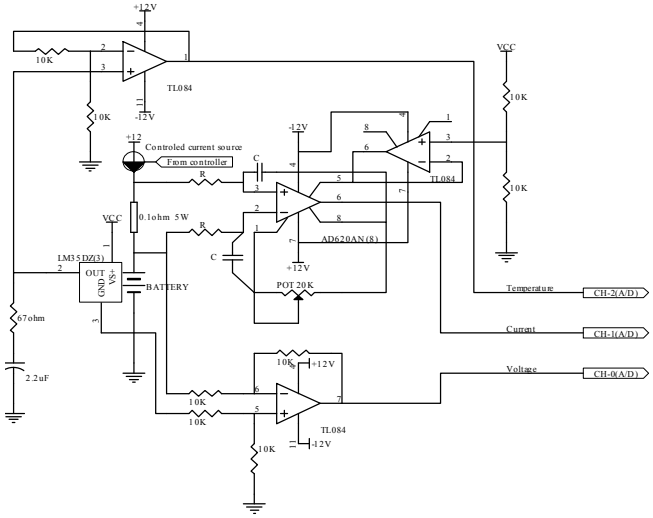

Fig. 4. Signal conditioning circuit

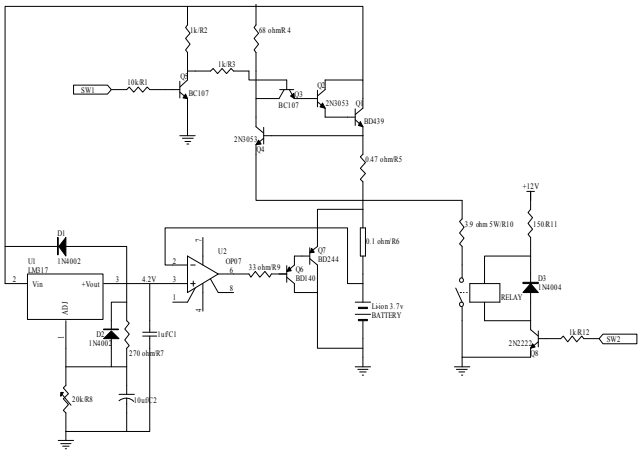

Fig. 5. Controllable charger circuit (driver) with voltage limiter

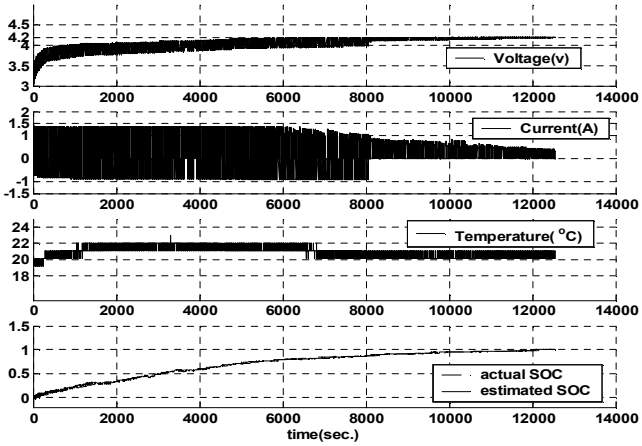

Fig. 6. The experimental data obtained from a full charging cycle of a 1.2Ah Li-Ion battery.

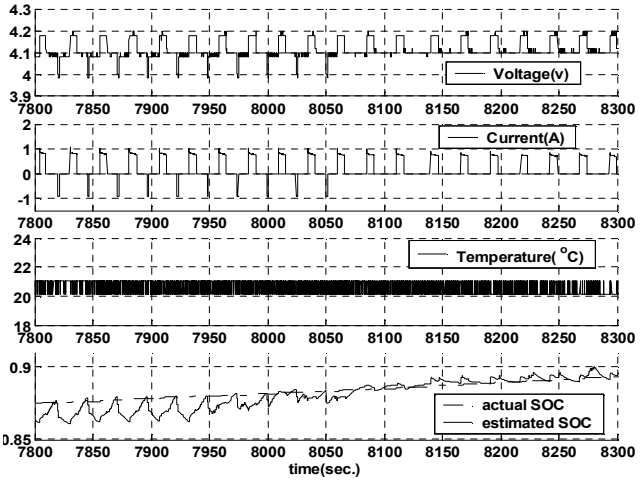

Fig. 7. 500 seconds of Fig. 6.

The covariance matrix **Q** is determined adaptively using (10) with initial value equal to $\mathrm{diag}[0.005 \quad 0.005]$. The variable N is selected equal to five. It is important to mention that the proposed algorithm is not very sensitive to the initial value of matrix **Q** and the parameter N. This is mainly due to the fact that matrix **Q** is adaptively adjusted to cope with the changes. The data in Fig. 6 are saved in the computer using the developed software. In order to show how the variables in Fig. 6 are varying with time, 500 seconds of Fig. 6 is shown in Fig. 7.

Since the neural network needs to be trained with different charging conditions, the entire charging cycle is divided into three parts: the first part is performed with 70% duty cycle, while the second part is carried out with 35% duty cycle, and the third part is performed with 20% duty cycle.

In order to avoid overtraining of the NN, 3600 samples are selected out of 240000 samples (i.e. 3 samples out of every 200 samples). The inputs to the neural network are $v(k-1)$, $i(k)$, and $\mathrm{SOC}(k)$, while the output is the battery terminal voltage at the present sample $v(k)$. There are 30 neurons in the hidden layer with $\sigma_i = 1.0$ $(i = 1,\ldots,30)$. These numbers are usually defined with trial and error [29]. At the end of the training phase, the performance index (i.e. sum of the squared errors) for all 3600 data is almost equal to 0.17.

Next, the trained neural network is used as a model in the EKF to estimate the same SOC shown in Fig. 6. The block diagram of the estimation algorithm is shown in Fig.8. The result of the SOC estimation is shown in Fig. 9. The RMS error (between the actual SOC and the estimated one) is equal to 2%, which can be considered as a good accuracy. Fig. 10 shows how the elements of the estimated covariance matrix for the system noise are varying during the SOC estimation.

B. Experimental Tests

Up to this point, training and testing of the RBF neural network (in conjunction with the EKF) are performed off-line. Next, the designed SOC estimator is tested in the controlled and on-line charging processes for the same lithium-ion battery. The results are shown in Figs. 11-14. Fig. 11 shows the battery terminal voltage, the charging current, the battery temperature, and the actual SOC waveforms. For clarity, 500 seconds of Fig. 11 is depicted in Fig. 12. Fig. 13

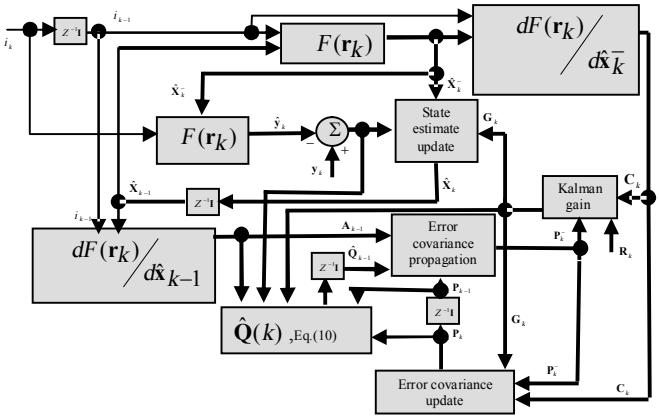

Fig. 8. Block diagram of the implemented estimation algorithms

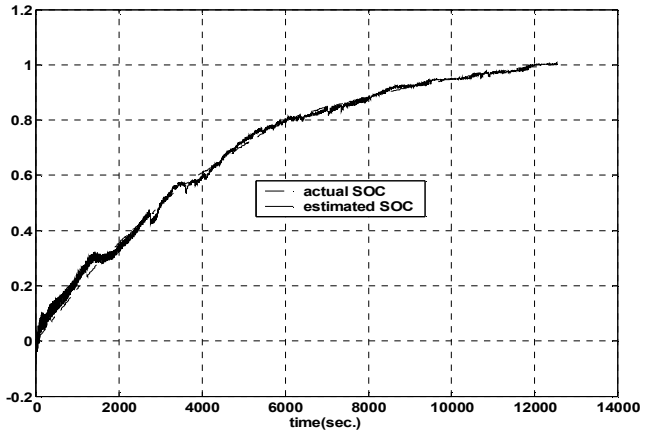

Fig. 9. The desired SOC measured by the Ampere-hour counting technique (dashed line) and the estimated SOC using the proposed method (solid line).

shows the actual and the estimated SOC during the entire charging process. The RMS error (between the actual SOC and the estimated SOC) is almost 3%. As Fig. 11 shows, at the beginning of the charging process, the reflex charging method has been used followed by the pulse charging technique (at about SOC=90%), in which the negative pulses have been eliminated for the remaining charging period.

Next, for testing the designed estimator with different initial conditions for the state variables, the battery is charged to about 65% of its nominal capacity. Then, it is separated from the charger and the charger is disconnected from the power supply for about 30 min. Next, the process of charging battery is resumed using the same initial conditions as if the battery were empty. The test results are shown in Figs. 14-18. As it is clear from Fig. 14, the estimated SOC converges quickly to the actual SOC in less than 2.5 min, which shows that the proposed estimator is robust against different initial conditions. The RMS error is almost 3% for this case. Figs. 15 and 16 show the battery terminal voltage, the charging current, the battery temperature, and the actual and the estimated SOC waveforms. Finally, Fig. 17 shows the variations in the elements of the covariance matrix **Q**.

Variations in Q_{21} at the beginning are indications of the quick reaction of the Kalman filter to reach the actual SOC. The experimental setup is shown in Fig. 18.

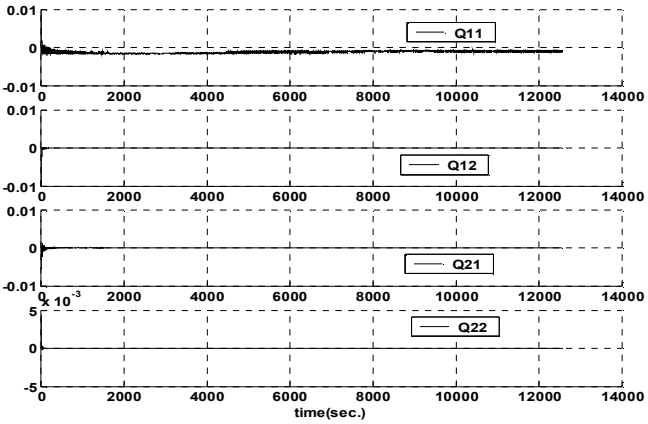

Fig. 10. Variations in the system noise covariance matrix **Q** using the adaptive procedure

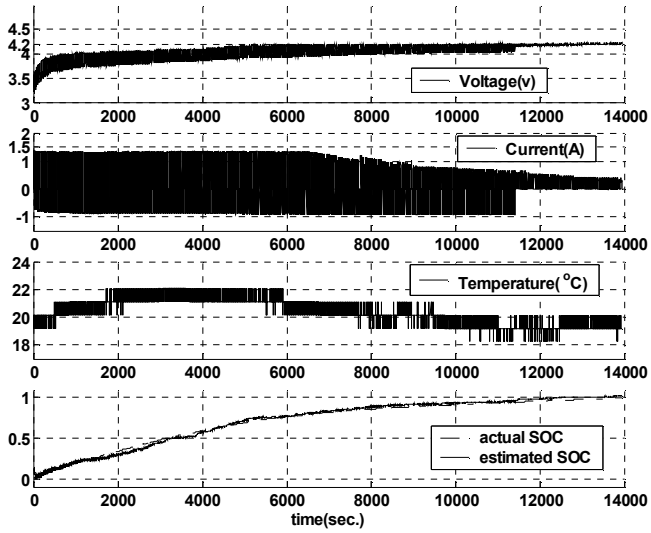

Fig. 11. Controlled battery charging using the proposed estimator.

V. Conclusion and Discussions

A SOC estimator for the lithium-ion batteries using neural networks and the extended Kalman filter with adaptive covariance matrix for system noise was proposed in this paper. The neural network is of RBF type and was trained off-line to find the appropriate model needed in the extended Kalman filter, which estimates the SOC of the battery. The experimental results of the proposed estimator showed good accuracy and fast convergence to the actual state variables, independent of the charging conditions and/or initialization of the Kalman filter. One important point is that the data for training the neural network was collected from a brand new and healthy battery. Hence, the trained neural network may not yield acceptable output when the battery ages. This problem can be resolved using data gathered throughout the lifetime of the battery. The other solution is to train the neural network adaptively with on-line data. These issues and the effect of the battery temperature on the SOC estimation and the charging current can give directions to the future works.

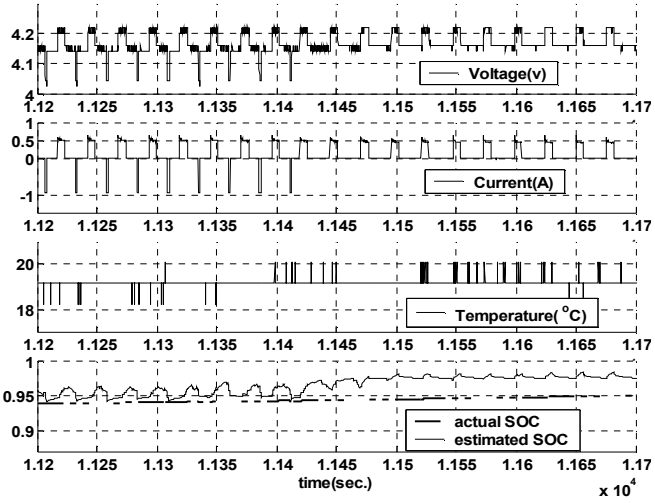

Fig. 12. 500 seconds of Fig. 11.

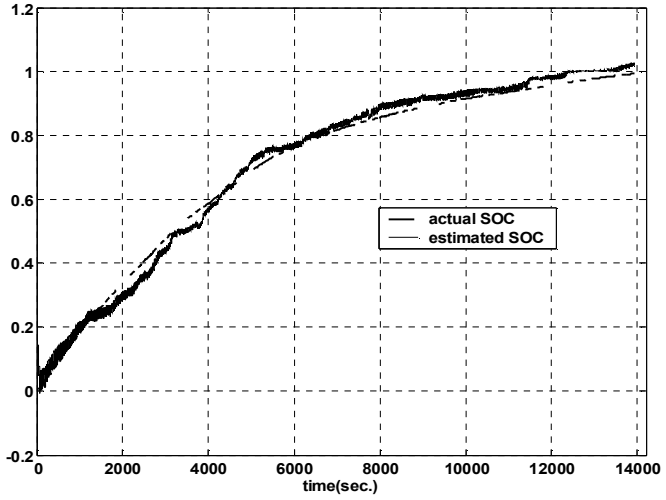

Fig.13. The actual and the estimated SOC during charging process, using the proposed estimator.

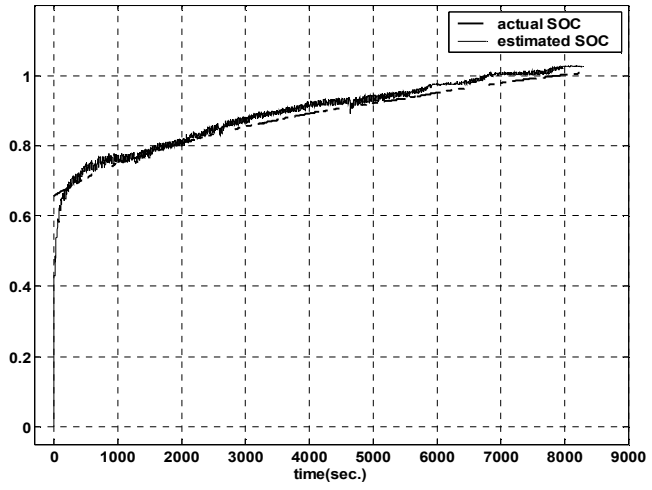

Fig. 14. Testing the proposed SOC estimator with different initial conditions for state variables of EKF (disconnecting the power supply for 30 min.).

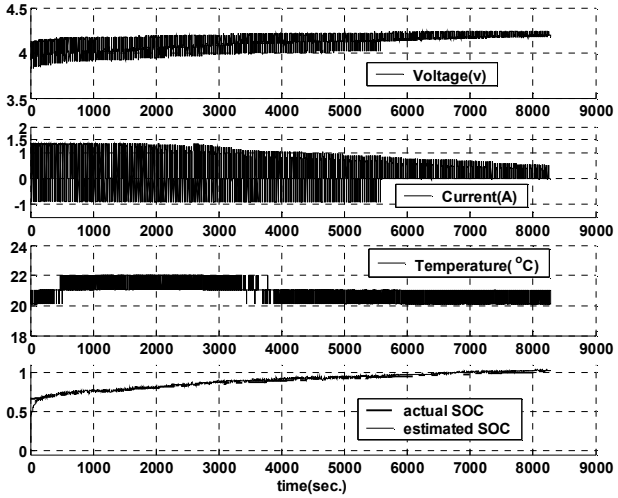

Fig. 15. Controlled battery charging using the proposed estimator.

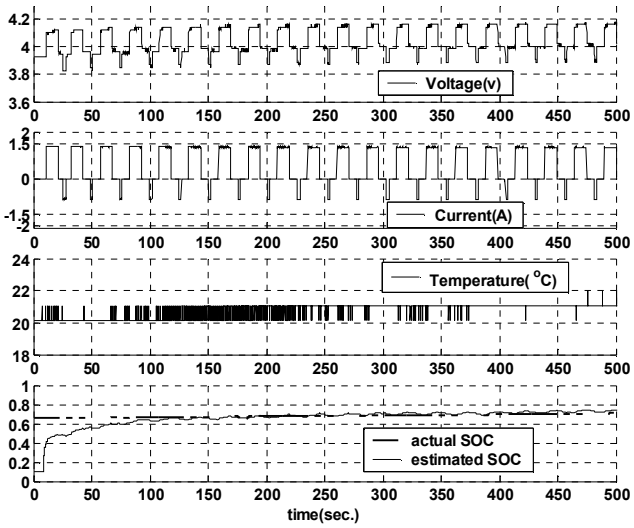

Fig.16: The first 500 seconds of Fig. 16.

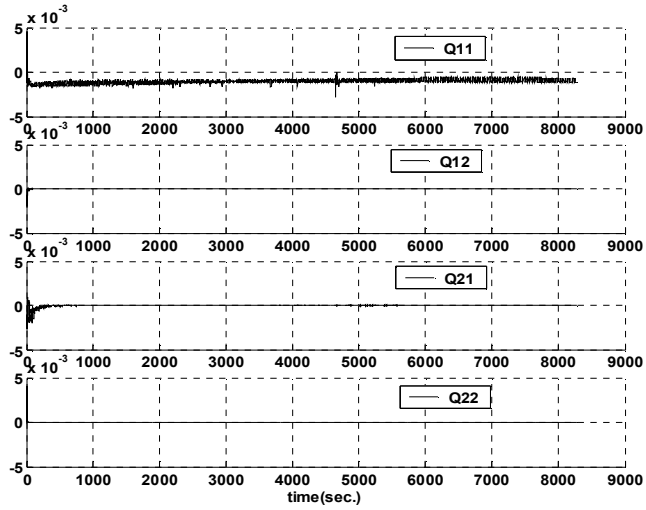

Fig. 17. Variations in the system noise covariance matrix **Q** using the adaptive procedure

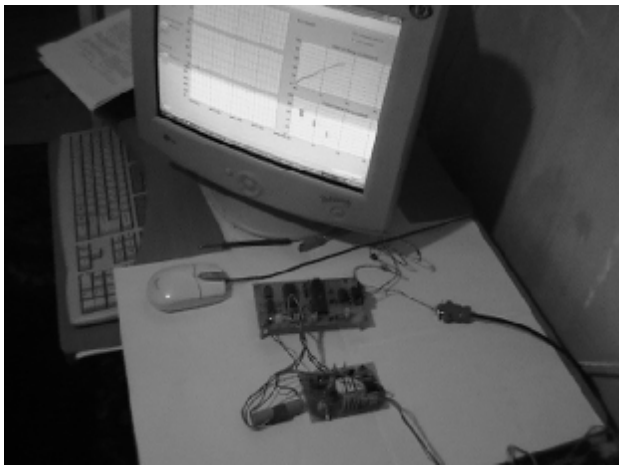

Fig. 18. The experimental setup

REFERENCES

[1] T.R. Crompton, *Battery Reference Book*, Newnes Publishing Co., Oxford 2000.

[2] S. Piller, M. Perrin, and A. Jossen, "Methods for state-of-charge determination and their applications," *J. Power Sources*, vol. 96, pp.113-120, 2001.

[3] E. Meissner and G. Richter, "Vehicle electric power systems are under changed! Implications for design, monitoring and management of automotive batteries," *J. Power Sources*, vol. 95, pp. 13-23, 2001.

[4] P. J. Blood and S. Sotiropoulos, "An electrochemical technique for state of charge (SOC) probing of positive lead–acid battery plates," *J. Power Sources*, vol. 110, pp. 96-106, 2002.

[5] G. C. Hsieh, L. R. Chen, and K. S. Huang, "Fuzzy-controlled li–ion battery charge system with active state-of-charge controller," *IEEE Trans. Ind. Electron.*, vol. 48, no. 3, pp. 585-593, June 2001.

[6] A. H. Anbuky and P. E. Pascoe, "VRLA battery state-of-charge estimation in telecommunication power systems, *IEEE Trans. Ind. Electron.*, vol. 47, no. 3, pp. 565-573, June 2000.

[7] F. Huet, "A review of impedance measurements for determination of state-of-charge or state-of-health of secondary batteries," *J. Power Sources*, vol. 70, pp.59-69, 1998.

[8] S. Rodrigues, N. Munichandraiah, and A.K. Shukla, "A review of state-of-charge indication of batteries by means of ac impedance measurements," *J. Power Sources*, vol. 87, pp.12-20, 2000.

[9] L. R. Chen, "Design of an optimal battery pulse charge system by frequency-varied technique, *IEEE Trans. Ind. Electron.*, vol. 54, no. 1, pp. 398-405, Feb. 2007.

[10] M. Coleman, C. K. Lee, C. Zhu, and W. G. Hurley, "State-of-charge determination from EMF voltage estimation: using impedance, terminal voltage, and current for lead-acid and lithium-ion batteries," *IEEE Trans. Ind. Electron.*, vol. 54, no. 5, pp. 2550-2557, Feb. 2007.

[11] A. J. Salkind, C. Fennie, P. Singh, T. Atwater, and D. E. Reisner, Determination of state-of-charge and state-of-health of batteries by fuzzy logic methodology, *J. Power Sources*, vol. 80, pp. 293-300, 1999.

[12] P. Singh, C. Fennie, and D. E. Reisner, "Fuzzy logic modeling of state-of-charge and available capacity of nickel/metal hydride batteries," *J. Power Sources*, vol. 136, pp.322-333, 2004.

[13] K. Kutluay, Y. Çadýrcý, Y. S. Özkazanç, and I. Çadýrcý, "A new online state-of-charge estimation and monitoring system for sealed lead–acid batteries in telecommunication power supplies, *IEEE Trans. Ind. Electron.*, vol. 52, no. 5, pp. 1315-1327, Oct. 2005.

[14] T. Yamazaki, K. Sakurai, and K. I. Muramoto, "Estimation of the recharge capacity of sealed lead-acid batteries by neural network," in *Proc. IEEE Int. Telecommus. Energy Conf*, San Francisco, 1998, pp. 210-214.

[15] J. Peng, Y. Chen, and R. Eberhart, "Battery pack state of charge estimator design using computational intelligence approaches," in *Proc. IEEE Annual Battery Applications Conf.*, Long Beach, U.S.A., 2000, pp. 173-177.

[16] C. H. Cal, D. Du, Z. Y. Liu, and H. Zhang, "Artificial neural network in estimation of battery state-of-charge (SOC) with nonconventional input variables selected by correlation analysis," in *Proc. IEEE Machine Learning and Cybern.*, Beijing, 2002, pp. 1619-1625.

[17] C. Cai, D. Du, Z. Liu, and J. Ge, "State-of-charge (SOC) estimation of high power NI-MH rechargeable battery with artificial neural network," in *Proc. IEEE Neural Inform. Proces.*, Singapore, 2002, pp. 824-828.

[18] C. H. Cai, D. Du, and Z. Y. Liu, "Battery state-of-charge (SOC) estimation using adaptive neuro-fuzzy inference system (ANFIS)," in *Proc. IEEE Int. Conf. Fuzzy Syst.*, St. Louis, pp.1068-1073, 2003.

[19] W. X. Shen, C. C. Chan, E. W. C. Lo, and K. T. Chau, "Adaptive neuro-fuzzy modeling of battery residual capacity for electric vehicles," *IEEE Trans. Ind. Electron.*, vol. 49, no. 3, pp. 677-684, June 2002.

[20] S. Pang, J. Farrell, J. Du, and M. Barth, "Battery state-of-charge estimation," in *Proc. ACC*, Arlington, 2001, pp. 1644-1649.

[21] B. S. Bhangu, P. Bentley, D. A. Stone, and C. M. Bingham, "Nonlinear observers for predicting state-of-charge and state-of-health of lead-acid batteries for hybrid-electric vehicles," *IEEE Trans Veh. Technol.*, vol. 54, no. 3, pp. 783-794, 2005.

[22] A. Vasebi , S.M.T. Bathaee, and M. Partovibakhsh, "Predicting state of charge of lead-acid batteries for hybrid electric vehicles by extended Kalman filter," *Energy Conversion and Management*, vol. 49, pp.75-82, 2008.

[23] O. Barbarisi, F. Vasca, and L. Glielmo, "State of charge Kalman fillter estimator for automotive batteries," *Control Eng. Practice*, vol. 14, pp.267-275, 2006.

[24] J. Lee, O. Nam, and B. H. Cho, "Li-ion battery SOC estimation method based on the reduced order extended Kalman filtering," *J. Power Sources*, vol. 174, pp. 9-15, 2007.

[25] S. Santhanagopalan and R. E. White, "Online estimation of the state of charge of a lithium ion cell," *J. Power Sources*, vol. 161, pp.1346-1355, 2006.

[26] G. L. Plett, Extended Kalman filtering for battery management systems of LiPB-based HEV battery packs, part 2: modeling and identification," *J. Power Sources*, vol. 134, pp. 262-276, 2004.

[27] G. L. Plett, Extended Kalman filtering for battery management systems of LiPB-based HEV battery packs, part 3: state and parameter estimation, *J. Power Sources*, vol. 134, pp.277-292, 2004.

[28] G. L. Plett, "Kalman-filter SOC estimation for LiPB HEV cells," in *Proc. 19th Int. Battery, Hybrid and Fuel Cell for Electric Veh. Symp. & Exhibition (EVS19)*, Bousan, 2002, pp. 1-12.

[29] S. Haykin, *Neural Networks: a Comprehensive Foundation*, Prentice Hall, New Jersey, 1994.

[30] S. Haykin, *Kalman Filtering and Neural Networks*, Wiley/Inter-Science, New York, 2001.

[31] P. S. Maybeck, *Stochastic Models, Estimation, and Control*, vol. 2, Academic Press, 1982.

[32] C. C. Hua and M. Y. Lin, "A study of charging control of lead-acid battery for electric vehicles," in *Proc. IEEE Int. Symp. Ind. Electron.*, Puebla, Mexico, 2000, vol. 1, pp. 135-140.